The variable stars in the compact halo globular cluster NGC 5634 visited again

A. Arellano Ferro [ORCID],[1]★ R. Michel,[2] M. A. Yepez,[3] S. Muneer,[4] I. Bustos Fierro [ORCID][5] and Z. Prudil[6]

[1]*Instituto de Astronomía, Universidad Nacional Autónoma de México, Ciudad de México, CP 04510, México*
[2]*Observatorio Astronómico, Nacional, Instituto de Astronomía, Universidad Nacional Autónoma de México, Carretera Tijuana-Ensenada Km. 107, Ensenada, B.C. 22860, Mexico*
[3]*Instituto Nacional de Astrofísica, Óptica y Electrónica (INAOE), Luis Enrique Erro No.1, Tonantzintla, Pue., C.P.72840, México*
[4]*Indian Institute of Astrophysics, Sarjapur Main Road, 2nd Block, Koramangala 560034, Bangalore, India*
[5]*Observatorio Astronómico, Universidad Nacional de Córdoba, Córdoba C.P. 5000, Argentina*
[6]*European Southern Observatory, Karl-Schwarzschild-Straße 2, D-85748 Garching, Germany*

ABSTRACT
We present new time-series CCD *VR* photometry of the globular cluster NGC 5634. We aim to use the known RR Lyrae stars, members of the cluster, as indicators of mean metallicity and distance. Accurate coordinates, periods, and an identification chart of the variables in the field of our images are provided. A membership analysis was performed, based on *Gaia*-DR3 proper motions, for 3525 point sources within 15 arcmin from the cluster centre. The membership status for each known variable was established and it was found that V10, V11, and V16 are most likely field stars. The variability of the RRab star V7, considered non-variable for a number of years, is demonstrated. Via the Fourier decomposition of the light curves of cluster member RR Lyrae, the mean metallicity and distance were calculated independently from RRab and RRc stars to find $[Fe/H]_{ZW} = -1.67 \pm 0.11$ y $D = 23.9 \pm 0.8$ kpc, and $[Fe/H]_{ZW} = -1.69 \pm 0.22$ y $D = 22.9 \pm 1.0$ kpc, respectively.

Key words: stars: horizontal branch – stars: variables: RR Lyrae – Galaxy: fundamental parameters – globular clusters: individual (NGC 5634).

1 INTRODUCTION

The globular cluster NGC 5634 (C1427-057 in the IAU nomenclature) ($\alpha = 14^h29^m37.23^s$, $\delta = -05°58'35.1''$, J2000; $l = 342.21°$, $b = +49.24°$) is a high galactic latitude outer halo object at some 25 kpc away from the Sun and about 21 kpc from the Galactic centre (Harris 1996). It has been scarcely studied in the past. It is a difficult target since there is a very bright foreground star at only ∼1.3 arcmin from the cluster centre, obliging to some manoeuvres to avoid it at the time of both the observations and reductions.

Based on its position and radial velocities, Bellazzini, Ferraro & Ibata (2002) have associated the cluster with the merging of the dwarf spheroidal galaxy Sagittarius with the Milky Way, suggesting that NGC 5634 was an original resident of the trapped galaxy. The cluster appears as a highly concentrated system. Its core and half-light radii (see Harris 1996), which at a distance of ∼25 kpc, are $R_c \sim 0.6$ pc and $R_h \sim 6$ pc, respectively, support the idea that the cluster lost its external halo due to tidal stripping forces (Salinas et al. 2005).

The population of variable stars in the field of NGC 5634 was discovered by Baade (1945) (V1–V7) and 60 yrs later by Salinas et al. (2005) (V8–V21). The positions and periods of these variables are listed in the Catalogue of variable stars of globular clusters (CVSGC; Clement et al. 2001).

There are reasons to pay a new visit to the small population of variable stars in this cluster; the coordinates listed in the CVSGC for some variables were based on relative (X,Y) positions measured on photographic plates, and an approximation of the cluster centre. Being such a compact and faint cluster and having nearly half of its variables buried deep in the central regions, it is clear that some variables are heavily blended, hence a reconsideration of their coordinates and variable type may be useful. At present we have access to new tools that facilitate the identification of the exact position of a variation, for instance one can perform a blinking of the full collection of astrometrically calibrated differential images to spot where the variations take place. Given the advent of accurate proper motions and parallaxes from *Gaia*-EDR3 (Lindegren et al. 2021), it has been shown by Prudil & Arellano Ferro (2024), based on the membership analysis performed for 170 globular clusters (Vasiliev & Baumgardt 2021), that some of those variables are in fact field stars (see also the membership flag in Clement et al. 2001). In the present paper, we shall report the results and caveats of our time series photometry, and we will perform a new stellar membership by an alternative approach. We shall produce and discuss a *V* versus *V − R* colour–magnitude diagram (CMD) and will use for the first time the recovered light curves of member variables towards
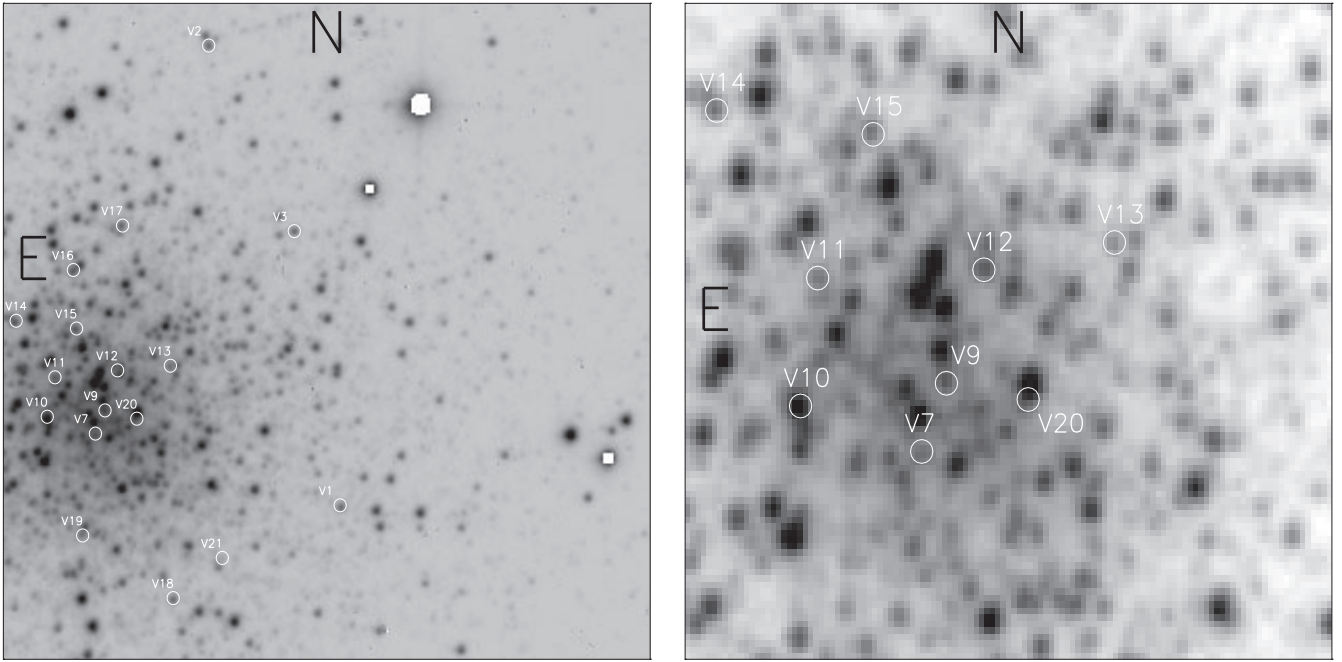
★ E-mail: armando@astro.unam.mx

Figure 1. Identification chart of the variable stars in the field of NGC 5634. The left panel is approximately 2.5 × 2.5 arcmin square. To facilitate the identification of the central region the panel to the right is about 0.45 × 0.45 arcmin square.

independent estimations of the metallicity and distance from their Fourier decomposition.

2 OBSERVATIONS AND IMAGE REDUCTIONS

2.1 Observations and reductions

All observations were performed with two telescopes; the 1.5m telescope in San Pedro Mártir Observatory, Baja California, Mexico, during five nights between 2024 May 1 and 11. The detector used was a 2048 × 2048 pixel CCD (e2v CCD-231-42) (Marconi 5) with an approximate scale of 0.493 arcsec per pixel after a binning of 2 × 2 pixels. A subarray of 700 × 700 pixels was used, for a field of approximately 3.45 × 3.45 arcmin square. Typical exposure times were 120–600 s in V and 80–120 s in R. The second telescope was the Himalayan Chandra 2.0m telescope of the Indian Astrophysical Observatory (IAO) at Hanle, India on 2024 March 3 and April 4. The telescope was equipped with an E2V CCD44-82-0-E93 detector (2048 × 4096) with a plate scale of 0.296 arcsec per pixel. A subarray of 1140 × 800 pixels was employed, corresponding to a field of view of about 5.6 × 3.9 arcmin square. Only a handful of V images were obtained with this instrument. Typical exposure times were 600 s in V.

For image photometric treatment, we employed the Difference Image Analysis (DIA) technique to extract photometry of all point sources in our images of the cluster. We used the *DanDIA* pipeline (Bramich 2008; Bramich et al. 2013, 2015), which has been described in detail by Bramich et al. (2011). The *DanDIA* pipeline creates a reference image for each filter by stacking a set of best-seeing images taken on a single night. A sequence of difference images was created by subtracting the reference image from each image in the time series collection. Differential fluxes are measured for each point source in the field, and instrumental light curves are built. The complete

process has been described in detail in section 2 of Arellano Ferro et al. (2008).

The presence of the ∼7 mag star HD 127 119 at about 1.3 arcmin of the cluster centre hinders the accurate photometry in the whole field of the cluster. To avoid contamination of our images by 'light bleeding', we decided to shift the cluster in the field of our images and leave the bright star off the chip. The price we had paid for this manoeuvre was not observing the variables V4, V6, and V8. The variable V5 was inadvertently lost at the southern edge of our field of observation. The remaining known variables are within our observed field and are identified in the ID chart in Fig. 1. The majority of the known variable stars are well within the half-light radius of the cluster.

2.2 Transformation to the standard system

The instrumental photometry was transformed to the standard Johnson–Kron–Cousins photometric system (Landolt 1992) *VR*, using local standard stars in the fields of the target clusters. These standard stars have been taken from the extensive collection of Stetson (2000).[1] We found 41 standard stars with instrumental light curves in the field of our images. The transformation of the instrumental light curves into the standard system was done independently for the SPM and Hanle data. Being our SPM data more abundant and taken under better seeing conditions, we a posteriority applied small offsets to the Hanle V data to match the SPM light curves. The colour $(v - r)$ dependence of the standard minus instrumental magnitudes, $V - v$ and $R - r$, are shown in Fig. 2 for the SPM data. The corresponding transformation equations are also given in the figure.
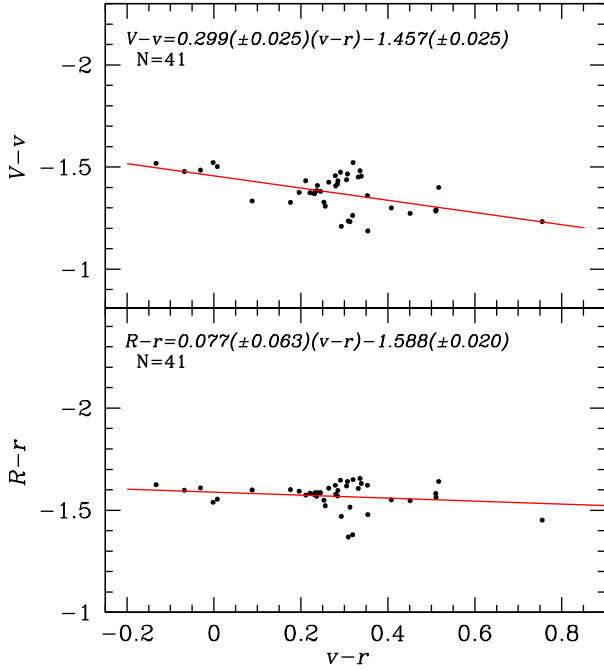
---

[1]https://www.canfar.net/storage/list/STETSON/Standards

Figure 2. Transformation relationship between instrumental and standard *V R* photometric systems. The transformations were defined employing 42 local standard stars from the collection of Stetson (2000).

3 STELLAR MEMBERSHIP ANALYSIS

We performed a stellar membership analysis in a grand field of NGC 5634, using for such an aim the high-quality proper motions available in the third data release of the *Gaia* mission (Gaia Collaboration 2023).

We used the method developed by Bustos Fierro & Calderón (2019) which is based on a two-step approach: (1) to find groups of stars with similar characteristics in the four-dimensional space of the gnomonic coordinates (X_t, Y_t) and proper motions ($\mu_{\alpha*}$, μ_δ) employing the BIRCH clustering algorithm (Zhang, Ramakrishnan & Livny 1996) and (2) in order to extract likely members that were missed in the first stage, the analysis of the projected distribution of stars with different proper motions around the mean proper motion of the cluster is performed.

The analysis was carried out on 3525 *Gaia* point sources within 15 arcmin from the centre of NGC 5634 and 1357 were found to be likely cluster members. The Vector Point Diagram (VPD) and the CMD are shown in Fig. 3, where field stars (grey dots) and cluster member stars (red dots) are distinguished. It is interesting to note that the farthest member is at about 4 arcmin from the cluster centre, which at a distance of about 23 kpc corresponds to a distance projected on the plane of the sky of about 27 pc confirming the compact nature of this halo cluster.

Before evaluating the cluster membership of the known variables, we revised their coordinates. We proceeded by blinking all our best quality differential images in small regions around each variable to confirm the temporal variation and the precise position of the blinking source. We noted some small differences with the coordinates published in the present edition of the CVSGC. In Table 1, we list all intensity-weighted mean magnitudes, amplitudes and periods for variables star measured in this study. We also include their coordinates and membership status.

From this membership analysis, we found that among the known variables V11 and V16 are likely field stars. The membership flag for variables in the CVSGC, that emerges from an independent membership analysis, (see Prudil & Arellano Ferro 2024), also indicates the field nature of V11 and V16. None the less, the two analyses disagree with respect to the nature of V20, but considering that this star is heavily blended, its membership status is indeed dubious. We shall return to the membership status of V20 in Sections 4.2 and 7.
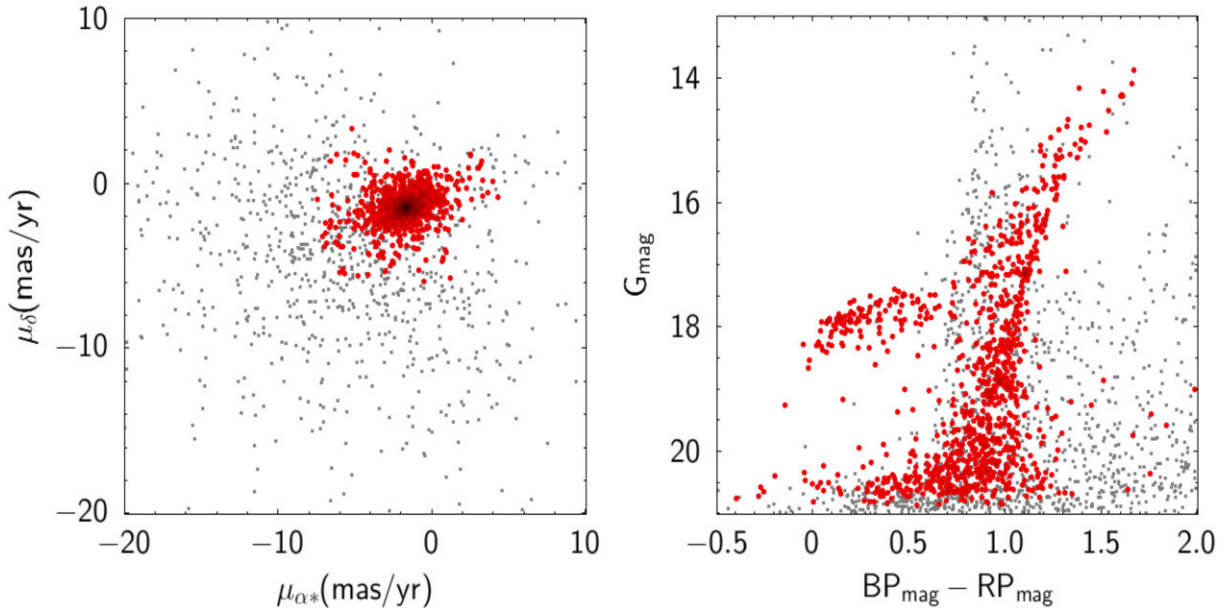

Figure 3. *Gaia*-DR3 VPD (left panel) and CMD (right panel) of the cluster NGC 5634. Red and grey points correspond to likely cluster members and field stars respectively, determined as described in Section 3. A total of 3525 *Gaia* point sources within 15 arcmin are displayed, while 1357, were found to be cluster members, all of them contained with a radius of 4 arcmin.

Table 1. General data of the variables in the FoV of NGC 5634.

Variable	*Gaia* ID	Type	$<V>$ (mag)	$<R>$ (mag)	A_V (mag)	A_R (mag)	Period (d)	HJD$_{max}$ (d + 2460000)	RA (J2000.0)	Dec. (J2000.0)	Membership (m/f)
V1	*3641359074110990464*	RRab	17.483	17.265	0.826	0.697	0.657848	0441.8987	14:29:33.51	−05:58:56.72	m
V2	*3641359275974954496*	RRab	17.657	17.430	1.331	1.085	0.605147	0441.9460	14:29:35.67	−05:57:14.83	m
V3	*3641359177190278528*	RRab	17.534	17.367	1.106	0.976	0.600419	0441.9433	14:29:34.30	−05:57:55.52	m
V4	*3641358902313485824*	RRc	17.617	–	0.481	–	0.385674	–	14:29:40.88	−05:59:43.98	m
V5	*3641355427683683456*	RRc	17.635	–	0.481	–	0.406517	–	14:29:36.38	−06:01:20.72	m
V6	*3641358902312004352*	RRc	17.637	–	0.519	–	0.344183	–	14:29:40.16	−05:59:31.19	m
V7	3641358971033097344	RRab	17.094	16.906	0.968	0.828	0.581274	0436.9661	14:29:37.23	−05:58:42.02	m
V8	*3641358902312006400*	RRc	17.653	–	0.547	–	0.330169	–	14:29:41.11	−05:59:16.63	m
V9	3641358971032981888	RRc	16.585	16.523	0.132	0.110	0.317521	0441.9460	14:29:37.12	−05:58:36.54	m
V10	3641358971032992768	RRab	15.1:	14.6:	–	–	–	–	14:29:37.99	−05:58:38.69	m
V11	3641358971033107072	RRab	17.118	16.788	0.827	0.506	0.663947	0403.8276	14:29:37.87	−05:58:29.39	f
V12	3641358971031515904	RRab	16.451	16.082	0.40	0.12:	0.624556	0441.9928	14:29:36.90	−05:58:28.38	m
V13	*3641359177191448064*	RRab	17.509	17.280	0.949	0.778	0.645648	0413.8012	14:29:36.15	−05:58:26.27	m
V14	3641358971031788672	RRab	–	17.543	–	0.785	0.725933	0434.8970	14:29:38.51	−05:58:17.38	m
V15	3641358971033084672	RRab	16.89:	17.000	–	0.338	0.859346	0441.8137	14:29:37.58	−05:58:18.75	m
V16	3641359211549981312	RRab	16.797	16.538	0.368	0.335	0.669811	0441.9873	14:29:37.66	−05:58:05.66	f
V17	*3641359211550005632*	RRc	17.509	17.317	0.421	0.334	0.405502	0441.8219	14:29:36.93	−05:57:55.30	m
V18	*3641358867952297600*	RRc	17.456	17.366	0.159	0.147	0.325762	0432.9253	14:29:36.02	−05:59:18.17	m
V19	3641358971031744640	RRc	17.477	17.403	0.082	0.073	0.295919	0441.8110	14:29:37.41	−05:59:04.12	m
V20	3641358971033060864	RRab	16.857	16.839	0.514	0.463	0.645748	0431.8422	14:29:36.64	−05:58:37.94	m[a]
V21	3641358867952534656	SX Phe	–	–	–	–	0.0666	0431.8422	14:29:35.29	−05:59:08.6	m
G1	*3641359177191556096*								14:29:35.10	−05:57:58.97	m
G2	*3641358867952547712*								14:29:35.00	−05:58:58.33	m
G3	*3641358971033104384*								14:29:38.17	−05:58:49.99	m
G4	*3641355947375985792*								14:29:43.16	−05:59:38.64	m
G5	*3641358971033112960*								14:29:39.92	−05:58:39.44	m
G6	*3641358971033056384*								14:29:36.88	−05:58:26.47	m

Notes. Stars with *Gaia* ID numbers in italics, are variables reported in *Gaia*-DR3.

Columns 3 and 4 are intensity-weighted mean magnitudes, columns 5 and 6 are light curves amplitudes. Column 11 indicates the cluster membership status; m – members, f – field.

[a]The membership status of V20 is discussed in Section 4.2.

4 VARIABLE STAR LIGHT CURVES RECOVERY AND CAVEATS

Most known variable stars in NGC 5634 are highly concentrated within the half-light radius of the cluster, and bad blending with multiple neighbours of similar magnitude or brighter is common. This anomalous circumstance, together with the image scale of our instruments and the poor seeing conditions that prevailed during some of our observing nights, prevented us from isolating and properly measuring some variables. In Fig. 4, we display the *VR* light curves of those stars we were able to measure during our best quality nights, which are colour-coded as described in the caption. In spite of the above limitations the displayed light curves are of quality enough to perform a Fourier decomposition analysis aimed at estimating the distance and metallicity, as shall be discussed later in this work.

All of our *VI* photometry for the studied variables in this work is provided in Table 2. A small portion of this table is given in the printed version of this paper and the full table is available in electronic form in the *Centre de Donnes astronomique de Strasbourg* data base (CDS).

At this point, a few comments on the variables V7 and V10 are in order.

V7 was discovered by Baade (1945) together with the other six variables V1–V6. V7 is the most central of the seven stars and while properly identified it was not measured. Later the star was not detected as variable by Salinas et al. (2005) and hence was listed as constant in the CVSGC. We have been able to

isolate and measure the star on the best sample of our images. The variability was confirmed using the same technique as Baade; the blinking comparison, but in this case of the many differential images built by DanDIA. The variation is conspicuous. The light curve is included in Fig. 4. The star is clearly a RRab star with amplitude modulations of the Blazhko type and has a period of 0.581274 d.

V10, on the other hand, was discovered by (Salinas et al. 2005) where the displayed light curve is clearly that of a RRab star. Using the blinking technique, we confirmed the variability at a position very similar to the one reported in the CVSGC. Unfortunately, DanDIA was unable to extract a proper light curve due to the extreme blending conditions at that point. However, the star residing at that position is very bright, the mean *VR* magnitudes place the star near the tip of the RGB in the CMD. Our conclusion is that if indeed we are dealing with an RRab star, then it is not a cluster member, but rather sits in front of the system.

4.1 Variables in the *Gaia*-DR3

The *Gaia*-DR3 reports 16 variables in the field of NGC 5634 and are included in Table 1 with their *Gaia* identification in italics. Ten of them match the known variables in the CVSGC. We found G, G_{BP} and G_{RP} light curves for six stars (Clementini et al. 2023); these correspond to the known RRab variables V2 and V3, and to the four RRc variables V4, V5, V6, and V8. Stars with *Gaia* ID number in bold font in Table 1 were missed by the *Gaia* mission because these
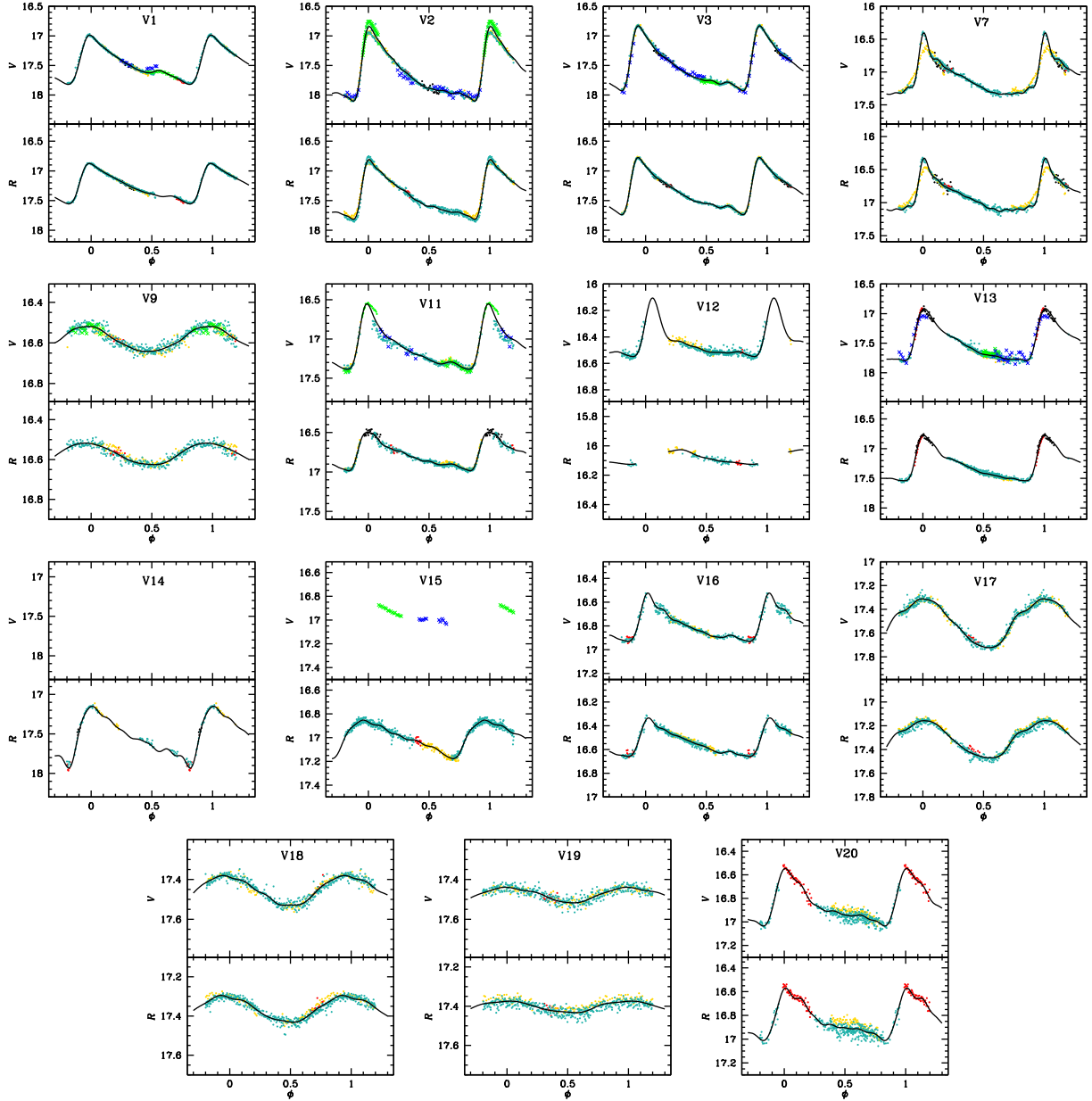
Figure 4. *V* and *R* light curves of variable stars in the field of NGC 5634. Colour code is as follows: red, yellow, and dark green dots are SPM data obtained between 2024 May 01 and 11. Green and blue crosses are *V* data obtained on March 14 and April 4 respectively, at the IAO.

stars are in the central region of the cluster, they are blended with brighter stars or are too faint.

As mentioned in Section 2, the RRc stars V4, V5, V6, and V8 are not in the field of our images. In order to include them in the Fourier decomposition analysis, we converted the *G*-band magnitudes into *V* band, using the correlations of Riello et al. (2021). These light curves are shown in Fig. 5. Their physical parameters will be presented in the following section.

The remaining six *Gaia* variables are listed in the bottom part of the table labelled 'G'. Stars G4 and G5 are outside the field of view of our images. G3 was not recovered by our photometry since it is badly blended and too close to the edge of our images. G1, G2, and G6, are declared as eclipsing binaries by *Gaia* and we do have photometry for the three of them. However, even employing our

best-quality data, i.e. the same sets used for the RR Lyrae in Fig. 4, we do not detect any variation in either of the three. Thus, we could not confirm their variation.

4.2 A brief comment on the Oosterhoff type of NGC 5634

With the estimated period and amplitudes for the RRab and RRc stars given in Table 1, the resulting log *P* – amplitude diagram, or Bailey's diagram, is displayed in Fig. 6 where the solid loci show the distribution of RRab and RRc stars in Oo II clusters, in opposition to the dashed loci typical of Oo I type clusters. The star distributions of NGC 5634 clearly identify the cluster as an Oo II. Three outstanding stars in the diagram are V7, V12, and V20 whose amplitudes seem smaller than expected. We found that very close to the position of

Table 2. Time-series *V* and *R* photometry for all the variables in the field of view of NGC 5634. (Full table is available in electronic format).

Variable Star ID	Filter	HJD (d)	M_{std} (mag)	σ_m (mag)
V1	V	2460403.79371	17.153	0.009
V1	V	2460403.79517	17.186	0.008
–	–	–	–	–
V1	R	2460413.76279	17.375	0.007
V1	R	2460413.76545	17.378	0.007
–	–	–	–	–
V2	V	2460403.79371	17.328	0.010
V2	V	2460403.79517	17.272	0.009
–	–	–	–	–
V2	R	2460431.83550	17.325	0.007
V2	R	2460431.83823	17.323	0.007
–	–	–	–	–
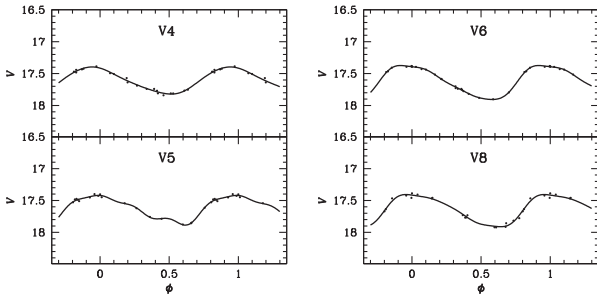
Figure 5. *Gaia G*-band light curves, converted into *V* band (Riello et al. 2021), of four RRc stars.
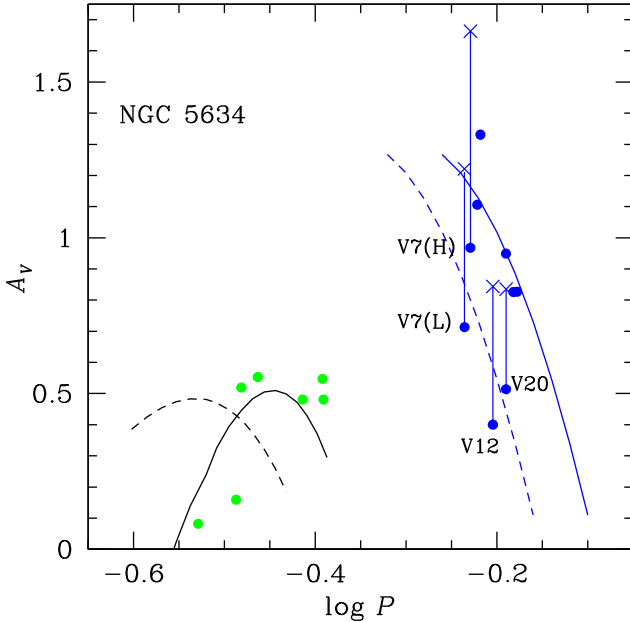
Figure 6. The period-amplitude or Bailey's diagram for NGC 5634. Blue and green symbols are used for RRab and RRc stars, respectively. Blue dashed and solid loci represent the distribution of unevolved and evolved RRab star typical of Oo I and Oo II clusters, respectively according to Cacciari, Corwin & Carney (2005). Black loci are the equivalent distributions for RRc according to Arellano Ferro et al. (2015) and Kunder et al. (2013). The star distribution clearly point NGC 5634 as an Oo II type cluster. The amplitudes of V7, V12, and V20 were corrected (blue crosses) for the presence of unresolved neighbours. See Section 4.2 for a discussion.

these variables, there are two *Gaia* stars with comparable brightness separated less than 1 arcsec, therefore unresolved in the ground-based observations. In the cases of V7 and V12 we have determined via a careful blinking of the residual images, that the actual variables are the brighter to the west and the fainter to the east of each pair, respectively. For the V20 pair, the variable is clearly the one to the south-east, whose light curve is that of a RRab with $V \sim 16.8$ mag (see Fig. 4). We calculated that V7 appears 0.580 mag brighter, V12 appears 0.559 mag brighter, and V20 0.524 mag brighter due to the blending with the unresolved neighbours. These corrections would place V7, V12, and V20 closer to the HB in the CMD (Fig. 7).

With the same assumptions, we also calculated that the actual amplitude of V12 should be 0.503 mag instead of 0.300 as measured (blended). However, the light curve of V12 is missing the maximum. We estimated its amplitude from a Fourier fit but it is possible that the amplitude has been underestimated. For V20 the amplitude should be about 0.835 mag instead of 0.514 (blended). Nevertheless, for V7, it should be noted that its light curve displays amplitude modulations (see Fig. 4), hence we corrected both the low and high extreme amplitudes for the presence of the unresolved companion, V7(L) and V7(H) in Fig. 6. These corrections would place them closer to the solid blue curve (Oo II cluster) in the Bailey's diagram.

The average periods for the RRab and RRc stars in Table 1 are: $< P_{ab} >= 0.66 \pm 0.08$ and $< P_c >= 0.35 \pm 0.074$ which also indicate that NGC 5634 is of the Oo II type. Another indicator of the Oosterhoff type in globular clusters is the frequency of RRc stars relative to the total number of RR Lyrae, i.e. NRRc/(NRRab + NRRc), for which, from the data in Table 1, we get 0.5. This clearly classifies the cluster as Oo II (Castellani, Caputo & Castellani 2003, see fig 5).

5 FOURIER DECOMPOSITION OF RR LYRAE LIGHT CURVES

The Fourier RR Lyrae light curve decomposition towards the estimation of stellar physical parameter is a well-established approach. The technique and the relevant semi-empirical calibrations for the calculation of metallicity, luminosity, radius and mass have been described in detail in the papers by Arellano Ferro (2022, 2024).

The light curve is fitted with a number of harmonics of the Fourier series model of the form:

$$m(t) = A_0 + \sum_{k=1}^{N} A_k \cos \left(\frac{2\pi}{P} k (t - E) + \phi_k \right), \quad (1)$$

where $m(t)$ is the magnitude at time t, P is the period, and E is the epoch. A linear minimization routine is used to derive the best-fitting values of the amplitudes A_k and phases ϕ_k of the sinusoidal components. From the amplitudes and phases of the harmonics in equation (1), the Fourier parameters, defined as $\phi_{ij} = j\phi_i - i\phi_j$, and $R_{ij} = A_i/A_j$, are computed. The Fourier coefficients are not specifically listed in this paper but they are available on request.

The low-order Fourier parameters can be used in combination with semi-empirical calibrations to calculate stellar values of [Fe/H], M_V, mass, and radius. The physical parameters for the measured RR Lyrae stars in NGC 5634 are listed in Table 3.

The average [Fe/H] and M_V (hence distance), should be representative of the parent cluster. The iron abundance is given in two scales, [Fe/H]$_{ZW}$, in the scale of Zinn & West (1984) which can be transformed into the spectroscopic scale of Carretta et al. (2009), via the equation; [Fe/H]$_{UVES} = -0.413 + 0.130$ [Fe/H]$_{ZW} - 0.356$ [Fe/H]$^2_{ZW}$.
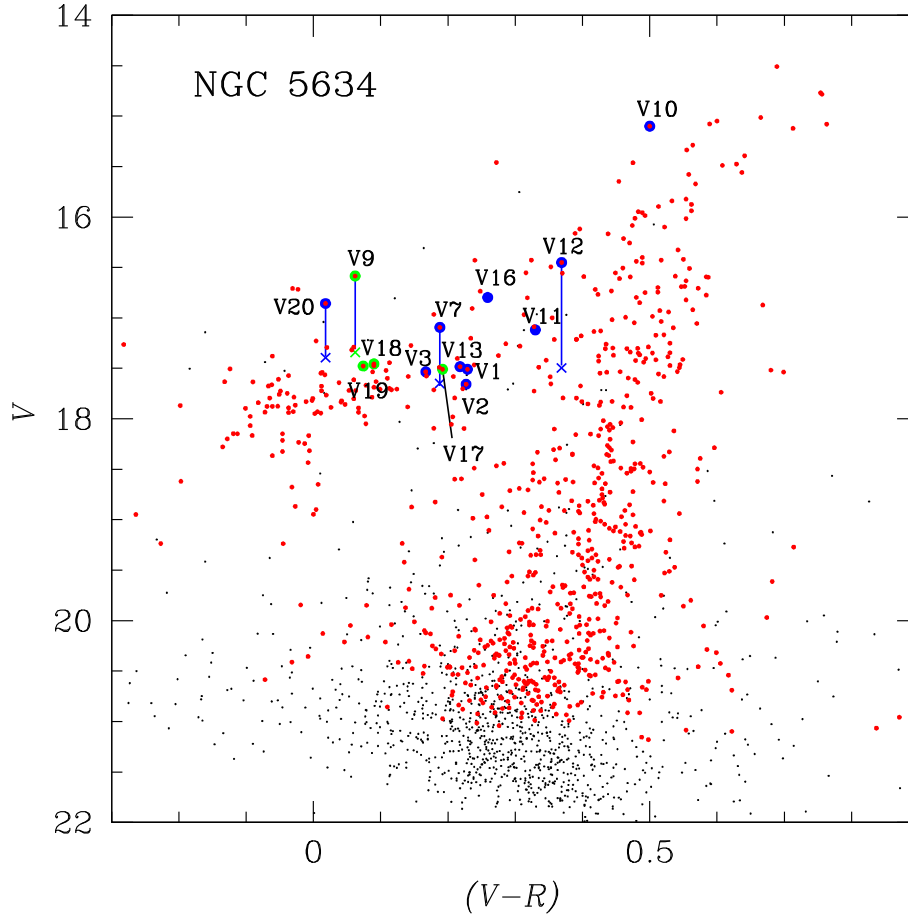
Figure 7. The NGC 5634 $V - (V - R)$ CMD. Red points are stars found as likely cluster members while grey dots represent the field star. Blue and green circles are used for RRab and RRc stars, respectively. Hence, cluster member variables have a red dot in the centre. Positions of the member stars V9, V12, V15, and V20, originally off the HB, could be corrected from the presence of a well identified close neighbour. The odd position of the apparently cluster member V10 could not be deblended. The Fourier physical parameters listed in Table 3 were calculated only for member stars in the HB.

Table 3. Physical parameters from the member RR Lyrae Fourier light curve decomposition.

ID	[Fe/H]$_{\rm ZW}$	[Fe/H]$_{\rm UVES}$	M_V	$\log T_{\rm eff}$	$\log(L/L_\odot)$	$M/M_\odot$	D(kpc)	$R/R_\odot$
				RRab				
V1	−1.50(3)	−1.41(3)	0.51(1)	3.80(1)	1.71(1)	0.66(7)	23.09(3)	5.94(1)
V2	−1.72(3)	−1.49(4)	0.44(1)	3.81(1)	1.74(1)	0.78(8)	25.53(6)	6.05(1)
V3	−1.67(3)	−1.63(3)	0.51(1)	3.81(1)	1.71(1)	0.73(7)	23.60(3)	5.86(1)
V7	−1.74(3)	−1.72(3)	0.59(1)	3.81(1)	1.68(1)	0.72(7)	24.34(3)	5.70(1)
V13	−1.83(4)	−1.84(5)	0.48(1)	3.80(1)	1.73(1)	0.74(8)	23.70(5)	6.13(1)
Weighted mean	−1.67	−1.62	0.52	3.80	1.71	0.72	23.85	5.89
σ	±0.11	±0.15	±0.05	±0.01	±0.01	±0.04	±0.84	±0.14
				RRc				
V4	−1.37(22)	−1.26(22)	0.56(4)	3.86(1)	1.68(1)	0.43(1)	24.00(54)	4.37(9)
V5	−2.07(8)	−2.20(12)	0.41(4)	3.85(1)	1.74(1)	0.54(1)	24.46(21)	4.93(9)
V6	−1.79(4)	−1.78(5)	0.54(2)	3.86(1)	1.68(1)	0.53(1)	24.46(20)	4.43(4)
V8	−1.79(9)	−1.78(12)	0.55(6)	3.86(1)	1.68(2)	0.55(4)	24.59(63)	4.40(11)
V17	−1.59(3)	−1.51(3)	0.46(1)	3.86(1)	1.72(1)	0.47(1)	24.03(12)	4.66(2)
V18	−1.67(17)	−1.62(20)	0.59(1)	3.86(1)	1.67(1)	0.52(3)	22.02(9)	4.28(2)
V19	−2.00(14)	−2.10(21)	0.59(3)	3.86(1)	1.67(1)	0.64(4)	22.22(16)	4.39(3)
Weighted mean	−1.69	−1.62	0.54	3.86	1.68	0.49	22.90	4.42
σ	±0.22	±0.30	±0.06	±0.01	±0.01	±0.01	±1.01	±0.25

Given the Galactic position of the cluster, it is subject to very low dust extinction. We have adopted $E(B - V) = 0.05$ (Harris 1996; Schlegel, Finkbeiner & Davis 1998; Schlafly & Finkbeiner 2011).

We found averages $[Fe/H]_{ZW} = -1.67 \pm 0.11$, $[Fe/H]_{UV} = -1.62 \pm 0.15$ and $D = 23.9 \pm 0.8$ kpc from the RRab light curves and $[Fe/H]_{ZW} = -1.69 \pm 0.22$, $[Fe/H]_{UV} = -1.62 \pm 0.30$ and $D = 22.9 \pm 1.0$ kpc from the RRc data. The results for the five RRab and seven RRc stars come from independent calibrations, obtained with different sets of calibrators, hence, results are also independent and agree very well. These values can be compared with the value quoted $[Fe/H]_{Spec} = -1.93 \pm 0.09$ in the spectroscopic scale (Carretta et al. 2009) and with the canonical value $[Fe/H] = -1.88$ listed by Harris (1996), and the mean distance $D = 25.959 \pm 0.62$ kpc estimated by Baumgardt & Vasiliev (2021). It is worth to note that the value of the metallicity reported by APOGEE DR17 (Schiavon et al. 2024) is $[Fe/H] = -1.72$, obtained for two cluster stars. Despite this, our results show a slightly metal richer and closer cluster, however we stress that the Fourier average results in Table 3 were limited to clear cluster members that are well placed on the Horizontal Branch as shall be shown in the following section.

6 THE COLOUR–MAGNITUDE DIAGRAM

The $V - (V - R)$ CMD of NGC 5634 is shown in Fig. 7. Red points are stars found as likely cluster members, while grey dots represent the field star. Blue and green circles are used for RRab and RRc stars, respectively. Hence, the cluster member variables have a red dot in the centre. The position of V10 is spurious; the star is blended, and we were unable to resolve it. The stars V7, V9, V12, V15, and V20, which according to their proper motions are likely cluster members, appear way above the HB, however, as discussed in Section 4.2 for V12 and V20, *Gaia* sources within 2 arcsec were also found for V7, V9, and V15. After correcting for the presence of unresolved neighbours for these five stars, they become closer to the HB (crosses in Fig. 7). Their corrected $<V>$ magnitudes were used in the calculation of their distance in the Fourier analysis in Section 5.

The Fourier physical parameters listed in Table 3 were calculated only for properly resolved cluster member RR Lyrae stars.

7 SUMMARY OF RESULTS

We were able to recover good light curves of some of the RR Lyrae in the field of NGC 5634, a few of them being well inside the central region of the cluster. A dedicated membership analysis employing the method of Bustos Fierro & Calderón (2019) and the independent analysis of Vasiliev & Baumgardt (2021) (see also Prudil & Arellano Ferro 2024) find that V11 and V16 do not pertain to the cluster. For V20 the two approaches find the star to be a member and a field star respectively. Membership methods are always subject to statistical considerations and may disagree on individual star, particularly in crowded regions, as it is the case of V20. This RRab star is badly blended with a brighter star which causes the star to appear brighter and with a smaller amplitude. Correcting by the presence of the contaminant star, V20 falls near to the HB and to the Oo II lucus on the Bailey's diagram. Thus we have classified the star as a likely cluster member.

The periods and equatorial coordinates of the variable stars have been refined and are reported in Table 1. The coordinates listed in the table correspond to the place where the detailed blinking comparison of the differential images marked the variations; they may differ a bit

from the coordinates listed in the CVSGC. Accurate identifications are given in the charts of Fig. 1.

The mean cluster iron abundance and distance found from independent calibrations of the Fourier decomposition parameters for the RRab and RRc stars light curves are $[Fe/H]_{ZW} = -1.68 \pm 0.18$, $[Fe/H]_{UV} = -1.62 \pm 0.26$ and $D = 23.4 \pm 0.9$ kpc.

DATA AVAILABILITY

The data employed in this work shall be available in electronic form in the Centre de Donnés astronomiques de Strasbourg data base (CDS), and can also be shared on request to the corresponding author.

REFERENCES

Arellano Ferro A., 2022, Rev. Mex. Astron. Astrofis., 58, 257
Arellano Ferro A., 2024, in de Grijs R., Whitelock P. A., Catelan M., eds, Proc. IAU Symp. 376, At the Crossroads of Astrophysics and Cosmology: Period-Luminosity Relations in the 2020s. Cambridge Univ. Press, Cambridge, p. 222
Arellano Ferro A., Giridhar S., Rojas López V., Figuera R., Bramich D. M., Rosenzweig P., 2008, Rev. Mex. Astron. Astrofis., 44, 365
Arellano Ferro A., Mancera Piña P. E., Bramich D. M., Giridhar S., Ahumada J. A., Kains N., Kuppuswamy K., 2015, MNRAS, 452, 727
Baade W., 1945, ApJ, 102, 17
Baumgardt H., Vasiliev E., 2021, MNRAS, 505, 5957
Bellazzini M., Ferraro F. R., Ibata R., 2002, AJ, 124, 915
Bramich D. M., 2008, MNRAS, 386, L77
Bramich D. M., Figuera Jaimes R., Giridhar S., Arellano Ferro A., 2011, MNRAS, 413, 1275
Bramich D. M. et al., 2013, MNRAS, 428, 2275
Bramich D. M., Bachelet E., Alsubai K. A., Mislis D., Parley N., 2015, A&A, 577, A108
Bustos Fierro I. H., Calderón J. H., 2019, MNRAS, 488, 3024
Cacciari C., Corwin T. M., Carney B. W., 2005, AJ, 129, 267
Carretta E., Bragaglia A., Gratton R., D'Orazi V., Lucatello S., 2009, A&A, 508, 695
Castellani M., Caputo F., Castellani V., 2003, A&A, 410, 871
Clement C. M. et al., 2001, AJ, 122, 2587
Clementini G. et al., 2023, A&A, 674, A18
Gaia Collaboration, 2023, A&A, 674, A1
Harris W. E., 1996, AJ, 112, 1487
Kunder A. et al., 2013, AJ, 146, 119

Landolt A. U., 1992, AJ, 104, 340
Lindegren L. et al., 2021, A&A, 649, A2
Prudil Z., Arellano Ferro A., 2024, MNRAS, 534, 3654
Riello M. et al., 2021, A&A, 649, A3
Salinas R., Catelan M., Smith H. A., Pritzl B. J., Borissova J., 2005, Inf. Bull. Var. Stars, 5640, 1
Schiavon R. P. et al., 2024, MNRAS, 528, 1393
Schlafly E. F., Finkbeiner D. P., 2011, ApJ, 737, 103

Schlegel D. J., Finkbeiner D. P., Davis M., 1998, ApJ, 500, 525
Stetson P. B., 2000, PASP, 112, 925
Vasiliev E., Baumgardt H., 2021, MNRAS, 505, 5978
Zhang T., Ramakrishnan R., Livny M., 1996, SIGMOD Rec., 25, 103
Zinn R., West M. J., 1984, ApJS, 55, 45

This paper has been typeset from a TEX/LATEX file prepared by the author.